buildings

MDPI

Article

Dynamic Characteristics of a 1950s Heritage Building: A Comparison of Original Design Methods and Modern Techniques

Fernando Peña * and Joel Ramos

Instituto de Ingeniería, Universidad Nacional Autónoma de México, Mexico City 04510, Mexico; jramosa@iingen.unam.mx

* Correspondence: fpem@pumas.iingen.unam.mx; Tel.: +52-555-623-3600

Abstract: Research on design rules and methods for architectural heritage is an important aspect of conservation practice. Nevertheless, efforts to recover and divulge design methods for Modern Heritage remain limited. This paper is related to the recent structural assessment of a 15-storey heritage building built in 1950, during which a document describing the original seismic analysis of this structure was identified. The methodology employed is of particular interest, as it involves the application of pioneer concepts of dynamic analysis in the design of the first tall buildings in Mexico. The primary aim of this paper is to review the seismic design criteria for the case under study in order to contribute to the state of the art in Modern Heritage. The review includes a comparison between the dynamic characteristics estimated during the design and the results of recent ambient vibration tests and numerical modeling. Several sources of error among the design criteria were identified. Notably, the fundamental period estimated during the design was 38% larger than the experimental value due to an underestimation in stiffness, which introduces significant uncertainty into the design. Overall, the review shows the evolution of seismic analysis over time and provide valuable insights for the study of similar buildings.

Keywords: existing buildings; modern heritage; 20th century heritage; structural assessment; dynamic properties estimation; ambient vibration testing

Citation: Peña, F.; Ramos, J. Dynamic Characteristics of a 1950s Heritage Building: A Comparison of Original Design Methods and Modern Techniques. *Buildings* **2024**, *14*, 2944. https://doi.org/10.3390/buildings14092944

Academic Editors: Haydee Blanco, Yosbel Boffill, Ignacio Lombillo and Alfonso Lozano

Received: 16 August 2024
Revised: 14 September 2024
Accepted: 16 September 2024
Published: 18 September 2024

1. Introduction

1.1. Problem Statement

The definition of conservation and restoration criteria for architectural heritage has gained important advances in the last decades. Examples of this are the publication of the ICOMOS principles and the ISCARSAH recommendations on the subject [1,2]. Among several key aspects from the engineering point of view, the observation of these criteria involves the need for a thorough understanding of the history of buildings to understand their present state [3]. Due to this reason, important efforts to recover and study ancient design rules and methods are continuously carried out [4–9]. Furthermore, design methods are sometimes compared to current methods or standards to study how these relate to each other [8–10]. An understanding of the original design and construction processes allows for an appreciation and recognition of the intrinsic or heritage value of the building, mainly the engineering value. In this context, the structural design and solution is an important heritage value that must first be recognized and then preserved, as it highlights the ancient building techniques and construction materials used in the past. The structure of the heritage buildings is, undoubtedly, an historical document of the abilities of the past builders [11].

Besides ancient structures, since the end of the last century, there has been a growing interest in the conservation of the architectural heritage of the 19th and 20th centuries [12–14], also named Modern Heritage [15]. This type of heritage involves several critical aspects,

among which are the following [13]: the difficulty of recognizing the building as part of the built heritage; the presence of new materials and construction techniques compared to ancient buildings; the difference in intervention criteria from classical conservation principles and the need to adapt these buildings to current structural safety requirements and existing regulations. Furthermore, Modern Heritage was often designed and constructed by using methods and techniques that are obsolete and forgotten nowadays. Although the actions to recover and divulge the structural analyses and design methods for these constructions should be recognized as equally important as the case of ancient heritage, only a few efforts can be found in the current literature [10,16]. Moreover, recent works discussing the seismic analysis and design methods of that time have not been identified.

The importance of the recovery of seismic design approaches can also be understood by keeping in mind that the first tall buildings, in the first half of 20th century, were designed when the bases of current analysis methods were not well established. In the context of Mexico City, seismic considerations for the design of tall buildings before the 1960s were essentially based on the criteria of more advanced engineers [17,18]. This was the case since the applicable code at that time [19] did not provide enough updated specifications for the seismic design.

1.2. Research Context and Aims

The structural assessment of a 15-storey heritage building located in Mexico City and built in 1950 was recently conducted. Following the international criteria for heritage conservation [1,2], a thorough search for information on design criteria and construction techniques was carried out. Among the information obtained, a publication that describes the methodology used during the design of the structure to calculate the equivalent seismic forces was identified [20]. The methodology is of interest and recognized as advanced for the time, as it involves the application of pioneer ideas about the dynamic analysis of structures [17,21]. It includes the calculation of natural vibration periods and maximum actions per story.

Given the existence of this information about early approaches for the dynamic design of buildings, the principal aim of this paper is to add to the state of the art in Modern Heritage by reviewing the criteria for the seismic design of the building. This information will be helpful for researchers and practitioners dealing with similar cases of study to understand the design criteria of that time. In addition, the secondary aims are to encourage divulgation regarding the design methods and construction techniques of Modern Heritage and show the evolution of seismic analysis over time. This last point is important, since according to [17], the tall buildings constructed in Mexico City in those years were designed according to the judgments of individual consultants and not following the provisions of the building code.

For the completeness of the review, a comparison between the dynamic characteristics obtained during the design and those obtained from recent ambient vibration tests is presented. In addition, numerical modeling is used to reproduce both the design and experimental results. This allows for a discussion of the criteria adopted for the design and a comparison between old and well-known modern techniques.

2. Case of Study

2.1. Description of the Building

The building is part of an architectural complex recognized by UNESCO as a World Heritage Site and is therefore of great cultural and historical importance. It can be identified as part of the Modern Architectural Movement due to its characteristics of an open ground story, frame-based structure, free facades and continuous windows (Figure 1). The main use of the building is for offices, libraries and auditoriums. The building has 15 floors and is 53.5 m high. The height of the floors is 3.5 m except for the first and last floors, which are 4.0 m high. The geometry of the plant is rectangular with dimensions of 17.0 $\times$ 53.0 m^2 in

the first 14 levels and of 12.3 × 3.6 m^2 in the last level (Figure 2). The dimensions of the plant in the transverse direction include 1 m long cantilevers at both ends.

The structure of the building is based on reinforced concrete moment frames, which are composed of 3 bays in the transverse direction and 13 bays in the longitudinal direction (Figure 3). The columns located in the A and D axes have circular cross-sections, while those in the B and C axes have rectangular cross-sections. The central bay in the transverse direction is composed of elements of the largest dimensions and has a shorter span than the outer bays. This was proposed in the original design to obtain a bay with high lateral stiffness that is capable of absorbing the totality of the lateral actions in the transverse direction [20].

The frame system of the structure is completed by masonry walls made of solid cement–sand pieces which enclose the stairs and elevators areas (Figure 2). There are also walls of hollow clay bricks that completely cover the north and south facades, except for the first floor. The facade walls are located next to the frames. As the cross-sections of the columns reduce in height, these walls have a variable separation from the frames for the upper floors. The building has an isolated footing foundation, since it was built on a rock site.

(**a**) (**b**)

Figure 1. Building under study: (**a**) northeast aerial view; (**b**) east facade.

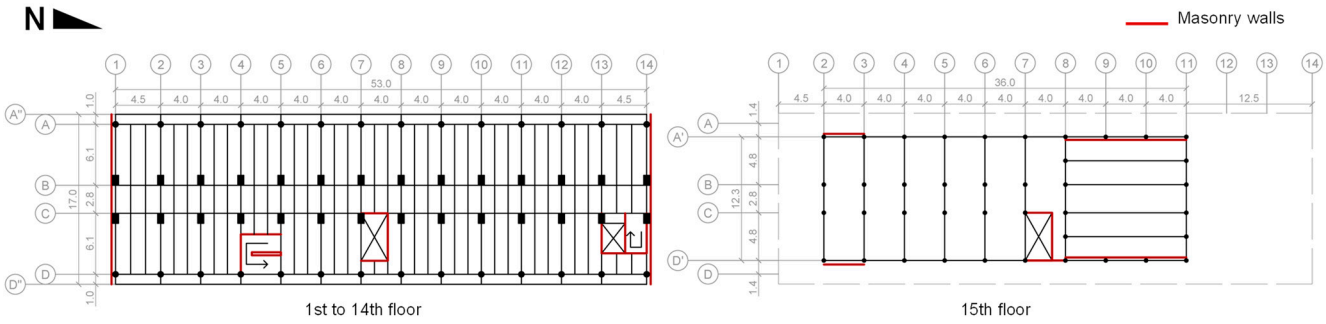

Figure 2. Structural plans of the building, dimensions in m.

The 15th floor of the structure can be considered as an appendix-like structure for its sudden change in geometry, which traduces to sudden changes in the mass and stiffness. All the columns on this floor have circular cross-sections. Also note that the columns located in the A′ and D′ axes are not continuous with the columns of the 14th floor (Figure 2). The transverse central bay in the appendix does not have elements of the largest dimensions, as is the case in the rest of the structure.

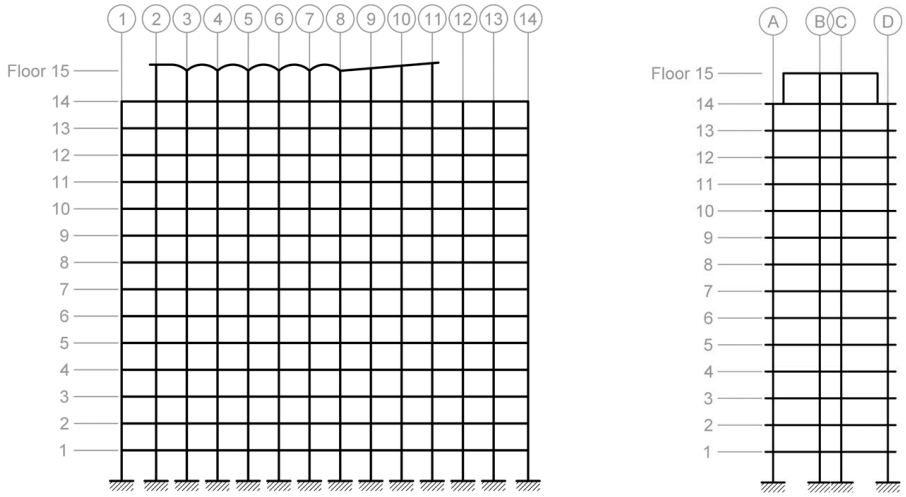

Figure 3. Typical frames of the structure: (**a**) longitudinal direction; (**b**) transverse direction.

The floor system in the first 14 levels is composed of a double slab forming a box section at each level (Figure 4). In the transverse direction, the box section has a different height for the central and extreme bays. It is 1.1 m high for the central bay and 0.5 m high for the outer bays. In this floor system, the longitudinal beams in the B and C axes are located at a different height than the other beams. This eccentric configuration allows for the differential height of the box section. In level 15, the roof system between 2 and 8 axes is based on barrel vaults, while the rest of the level is covered with a solid slab.

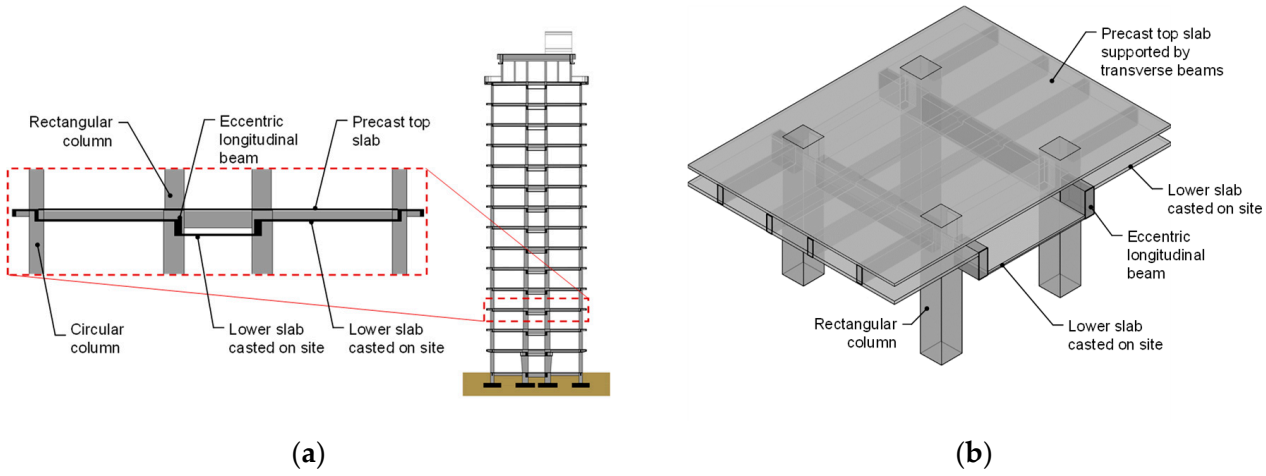

Figure 4. Representations of floor system: (**a**) transverse view; (**b**) 3D view.

2.2. Information Gathering for the Structural Assessment

In the context of the structural assessment carried out, searching for information was essential to study the structural behavior and the diagnosis of the current state of the building. The search included historical research, site visits and surveys, as well as the performance of several structural tests.

From an exhaustive search of the available information, it was possible to identify and collect original architectural and structural drawings, a study on the soil mechanics of the site, historical photos, general data about the construction of the building and the publication that describes the seismic analysis of the structure [20]. It is noteworthy that structural drawings lost their legibility, and thorough work to recover and preserve the information was needed. Furthermore, seismic antecedents of the building were investigated. Although the structure has been subjected to strong ground motions, it has

been concluded that the overtime behavior of the building is correct in terms of the safety of its users.

The current state of the building was primarily investigated via several site visits and surveys. This allowed us to review or update the information obtained from original drawings, identify the current uses of the building, define the gravitational loads and observe the state of the structural elements. Visual inspections were completed with the use of a drone and LiDAR scans. It should be pointed out that differences in the dimensions of the structural elements were identified from those reported in the seismic analysis. As an example, the dimensions of columns are compared in Table 1. One can observe that the measured cross-sections are larger than those considered for the seismic analysis.

Table 1. Dimensions of columns from original seismic analysis [20] and field measurements, in mm.

Story	Rectangular Columns (Longitudinal × Transverse Dimensions)		Circular Columns (Diameter)	
	Design	Measured	Design	Measured
1	600 × 900	600 × 1000	450	550
2	600 × 800	600 × 900	450	550
3	600 × 800	600 × 850	450	500
4	600 × 600	600 × 800	400	500
5	600 × 600	600 × 750	400	500
6	600 × 600	600 × 700	400	450
7	500 × 500	600 × 650	350	450
8	500 × 500	600 × 650	350	450
9	500 × 500	600 × 600	350	400
10	450 × 450	500 × 550	300	400
11	400 × 400	500 × 450	300	350
12	350 × 350	400 × 450	300	350
13	350 × 350	400 × 400	250	350
14	300 × 300	350 × 350	250	350
15	300 × 300	-	-	350

The structural tests carried out included the following: ambient vibration tests, concrete samples extractions, reinforcement steel scanning and the exposure of reinforcement steel in concrete elements. The results of these tests, complemented with visual inspections, allowed us to confirm the good condition of the structural elements. Additionally, the results were the basis for defining the mechanical properties of the materials.

3. Design Methods

The seismic analysis approach, which was used to obtain the maximum values of the story shears due to seismic actions, is recognized as advanced for its time, since the Mexican Code only used to establish seismic coefficients according to the type of construction [19]. Moreover, these coefficients were of constant application for all the floors of a building. The analysis was mainly based on the theory of seismic wave transmission inside buildings [21]. This theory has been recognized as a pioneer work on the dynamic analysis of buildings that influenced the engineering practice in Mexico [17]. The application of these ideas implied obtaining the vibration periods of the structure, as well as idealizing the ground motion as a harmonic signal, which, in turn, was defined by some period or frequency value and the maximum ground acceleration for the site. It is worth noting that all the involved procedures consisted of hand calculations.

The structure was idealized as a classical multiple-degree-of-freedom system where the mass of the building was lumped at its floors, and only horizontal displacements were considered; the lateral stiffness of each story was represented by a spring. For the mass calculation, the weight of the double slab at each level (box section) was considered as 4.0 kN/m^2. Live loads were defined according to the use of the spaces and the specifications of the Mexican Code (Table 2) [19]. Loads for facade walls, interior walls and facade

windows were also considered, but it is not clear if the self-weight of the structural elements was taken into account. The mass values per floor are shown in Table 3.

Table 2. Uses considered for the design of the structure and live loads according to [19].

Use	Load, kN/m^2
Office	2.0
Library	3.0
Stair	5.5
Conference hall	3.5
Rooftop	1.0

Table 3. Mass and lateral stiffness from the original seismic analysis of the structure [20].

Floor (for Mass) Story (for Stiffness)	Mass, kg	Stiffness in Longitudinal Direction, kN/mm	Stiffness in Transverse Direction, kN/mm
1	913,000	1662	1932
2	884,000	944	1070
3	864,000	802	951
4	861,000	737	729
5	850,000	699	714
6	810,000	621	666
7	785,000	420	465
8	785,000	398	452
9	770,000	374	420
10	750,000	247	298
11	760,000	189	220
12	765,000	153	148
13	743,000	97	90
14	757,000	97	88
15	413,000	66	65

3.1. Estimation of Dynamic Properties

The method used to calculate the fundamental period in the main directions of the structure was proposed by Newmark [22]. In this numerical method, the period can be calculated by successive approximations based on an initial-proposed deformed configuration of the structure. As a result of the procedure, the modal shape is also obtained. The original calculations to obtain the first mode in the longitudinal direction are shown in Figure 5a.

The story lateral stiffnesses in the longitudinal direction, required for the application of the method of Newmark, were calculated using Equation (1), as proposed by Wilbur [20], where k_n is the story stiffness of the n story, E is the elasticity modulus of the material, h is the story height, K_{co} is the inertia-to-length relation of each column, K_{ga} is the inertia-to-length relation of each upper beam of the story, and K_{gb} is the inertia-to-length relation of each lower beam of the story. Given that the structure was considered fixed at its base, for the first story stiffness, the sum of K_{gb} was considered as an immense value, so the inverse of this sum was equal to zero. It is worth noting that Equation (1) is applicable to 2D regular frames composed of elements with the same moment of inertia per level and for structures where axial deformations can be neglected. The total lateral stiffness of the structure in this direction was obtained as the sum of the lateral stiffness of each frame. The lateral stiffness values obtained are shown in Table 2.

$$k_n = \frac{24E}{h_n^2\left(\frac{2}{\sum K_{co}} + \frac{1}{\sum K_{ga}} + \frac{1}{\sum K_{gb}}\right)} \quad (1)$$

(**a**)

(**b**)

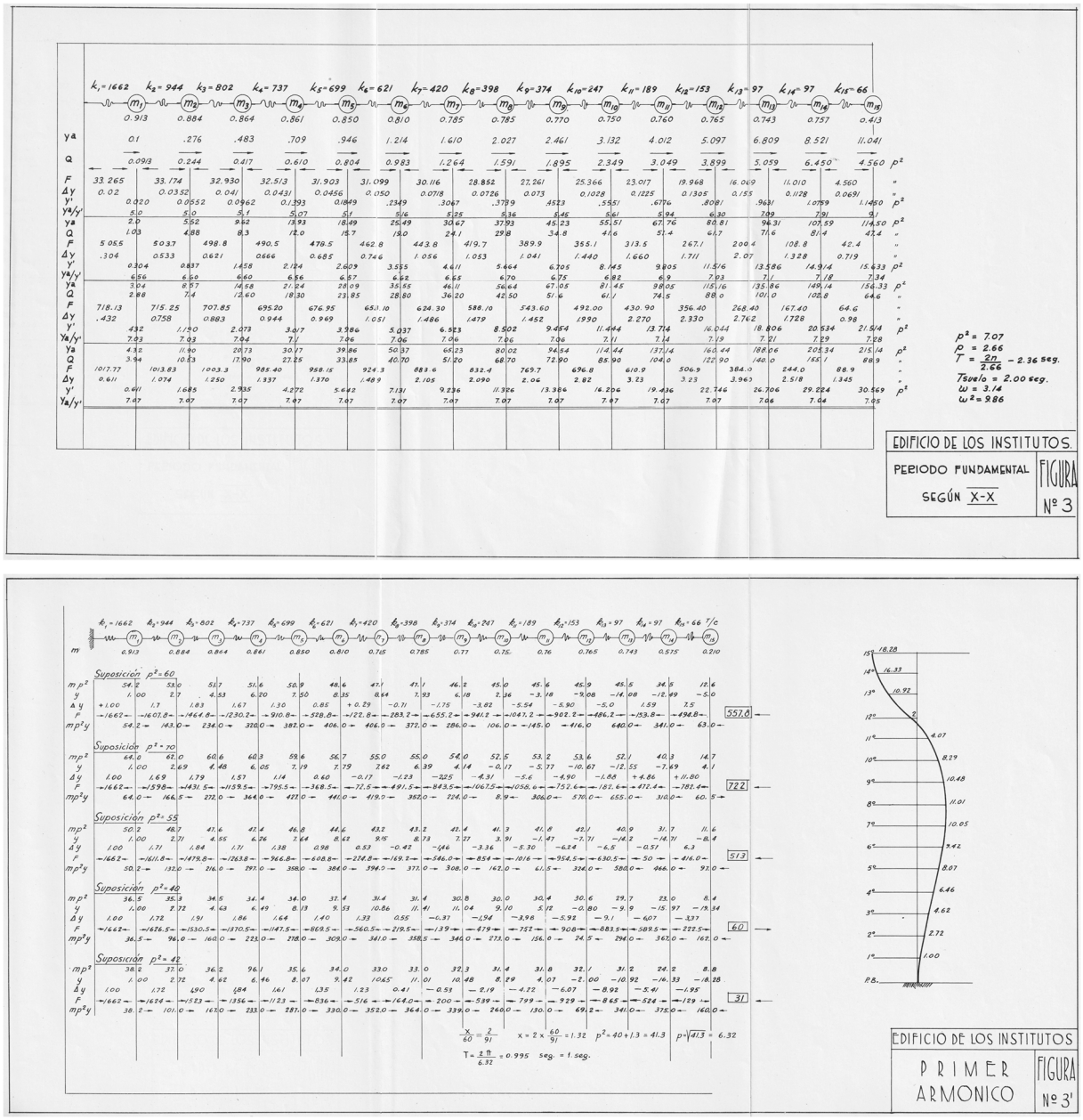

Figure 5. Original calculations to estimate the vibration modes in the longitudinal direction [20]: (**a**) first mode; (**b**) second mode.

The second longitudinal vibration period was also calculated. In this case, the method of Holzer [23] was used, which is a trial-and-error method for obtaining higher vibration modes. The first step in the method is to propose the value of the circular frequency of the mode. As the frequency is unknown, the procedure can result in a higher mode than desired. However, the mode can be identified using the modal shape obtained and the number of inflection points. The original calculations to obtain this mode are shown in Figure 5b.

For the first transverse period estimation, a slightly different treatment was needed given that Equation (1) was not applicable. In this direction, the frames are irregular because of the bays with different spans and the elements with different cross-sections and, therefore, different inertias. The procedure started by assuming a reasonable lateral force distribution. Then, an approximated method based on moment distribution was used to obtain the internal forces in the elements of a typical transverse frame [24]. Using

the moments and stiffness of the columns located in the B and C axes, the lateral frame displacements were also calculated by means of the successive approximations method proposed by Newmark. Once these displacements were obtained, the story stiffnesses of the frame were calculated (Table 3). Finally, the method of Newmark was again applied to obtain the fundamental transverse period and modal shape. It can be noted that the total lateral stiffnesses in both directions are similar. Here, the total lateral stiffness was calculated as the sum of each single frame in each direction.

It is worth noting that an elasticity modulus E_c of 20,000 MPa (200,000 kg/cm^2) was used to calculate the lateral stiffnesses of the structure. The Mexican Code applicable during the design [19] provides Equation (2) for E_c, where it is common to express the concrete compressive strength f'_c in kg/cm^2. A common assumption in the early 20th century in the design of concrete structures was that the calculus of the elasticity modulus of concrete was proportional to the compressive strength [25] instead of being proportional to the square root of the compressive strength, as is nowadays considered (see Equation (3)).

Based on the specified compressive strength for the building, which is 21 MPa (210 kg/cm^2), an E_c value close to the design value is obtained using Equation (2) (210,000 kg/cm^2). This elasticity modulus is considerably different from the current Mexico City Code [26] that proposes Equation (3) for Class 2 concrete, in kg/cm^2. From Equation (3), we obtained an E_c value of 11,593 MPa (115,931 kg/cm^2) for the same f'_c, which is approximately 60% of the design value. From the theory of structural dynamics, the period of a system is inversely proportional to the square root of its lateral stiffness. Based on the above, it can be demonstrated that periods from design methods increase approximately 30% if the value of E_c that is calculated using Equation (3) is used; that is, the structure becomes more flexible.

$$E_c = 1\,000 f'_c, \text{ in kg/cm}^2 \tag{2}$$

$$E_c = 8\,000 \sqrt{f'_c}, \text{ in kg/cm}^2 \tag{3}$$

The obtained periods are shown in Table 4. Note that in agreement with the lateral stiffness estimation, the same period value was found in both directions for the first mode. It must be highlighted that in these calculations, only the stiffness of the frame system was considered; the stiffness of the masonry walls was not included.

Table 4. Vibration frequencies and periods from the original seismic analysis of the structure [20].

Mode	Vibration Frequencies (Hz)		Vibration Periods (s)	
	Longitudinal Direction (L)	Transverse Direction (T)	Longitudinal Direction (L)	Transverse Direction (T)
1	0.424	0.424	2.36	2.36
2	1.006	-	1.00	-

3.2. Calculation of Story Shears

Consider an idealized shear structure with constant weight and lateral stiffness per unit of height. According to [21], the relationship between the horizontal deformations of the structure and time can be expressed using differential Equation (4), where t is time, x is the vertical position inside the building, c is the weight of the building per unit of length, g is the gravity acceleration, and K is the lateral stiffness defined by Equation (5), where, in turn, S is the story shear. Note that these expressions imply that the deformed shape of the structure and its story shear can be represented by continuous functions.

$$K \frac{\delta^2 y}{\delta x^2} = \frac{c}{g} \frac{\delta^2 y}{\delta t^2} \tag{4}$$

$$K = S \frac{\delta x}{\delta y} \tag{5}$$

The solution of Equation (4) can be expressed as Equation (6), in which f is any function two-times derivable. In addition, by means of Equations (5) and (6), we can obtain Equation (7) for S. Respectively, (6) and (7) represent the horizontal deformation and the story shear wave at the interior of the building caused by a motion wave f applied at its base.

$$y = f\left(t \pm \frac{x}{\sqrt{Kg/c}}\right) \tag{6}$$

$$S = \pm\sqrt{\frac{Kc}{g}} f'\left(t \pm \frac{x}{\sqrt{Kg/c}}\right) \tag{7}$$

If the ground motion y_0 is considered as the cosine function (Equation (8)) with period T and circular frequency ω, then the shear wave at the base of the structure S_0 is defined by Equation (9). By evaluating (9) with x equal to zero and t equal to $T/4$, Equation (10) is obtained, which is the maximum amplitude of the shear wave at the base of the structure. It can be proved that (10) can be expressed in terms of the weight of the first floor C and the lateral stiffness of the first story k, as is shown in Equation (11). This equation allows us to calculate the shear applied at the base of a structure. Note that for some specific structure, the magnitude of the force is only proportional to the term $a\omega$.

$$f = y_0 = a(1 - \cos \omega t) \tag{8}$$

$$S_0 = -\sqrt{\frac{Kc}{g}} a\omega \sin\left[\omega\left(t - \frac{x}{\sqrt{Kg/c}}\right)\right] \tag{9}$$

$$S_0(x = 0, t = T/4) = a\omega\sqrt{\frac{Kc}{g}} \tag{10}$$

$$S_0 = a\omega\sqrt{\frac{kC}{g}} \tag{11}$$

The theory described and Equation (11) were the bases for the calculation of story shears [20]. The required process can be divided into two parts: first, the definition of the force at the base of the structure; second, the analysis of the superposition of shear waves within the structure for the calculation of the maximum shear at each story.

According to [20], ground motions with periods up to two seconds produce significant accelerations. It is also said that the data available in Mexico at that time indicated that the maximum accelerations were related to motions with a period of one second. Based on these ideas, it was assumed that the maximum ground acceleration could be $g/40$ or $g/80$ for motions with a period of one or two seconds, respectively. The definition of these values was perhaps supported by the seismic coefficients of the Mexican Code [19], since it established a coefficient equal to $g/40$ for office buildings. From the theory of structural dynamics, the pseudo-acceleration of a single-degree-of-freedom system is equal to the displacement times the square of the circular frequency, that is, the term $a\omega^2$. Using this equality, the two maximum ground accelerations gave a value of 0.0389 m/s for the term $a\omega$. Then, from the mass and stiffness of the first floor/story of the structure, a value of 1 530 kN was finally obtained for S_0. This S_0 value was used only for the longitudinal direction analysis. For the transverse direction, S_0 was reduced 40%. The reason for this reduction was not explained in [20].

The assumptions for the shear transmission within the structure are resumed in Figure 6 [20,21]. The origin of the shear waves in each level is aligned on a line with a slope equal to the velocity of the wave transmission. When the wave reaches the top of the structure, it is reflected downwards with a negative sign, since the shear at the free end must be zero. Then, when the wave reaches the base of the structure, it is reflected with the same sign. Note that the wave cycle starts again after the second arrival at the base of the

structure. The duration of one cycle is equal to the period of the structure, T_s, and therefore, the velocity of the wave transmission is $4H/T_s$.

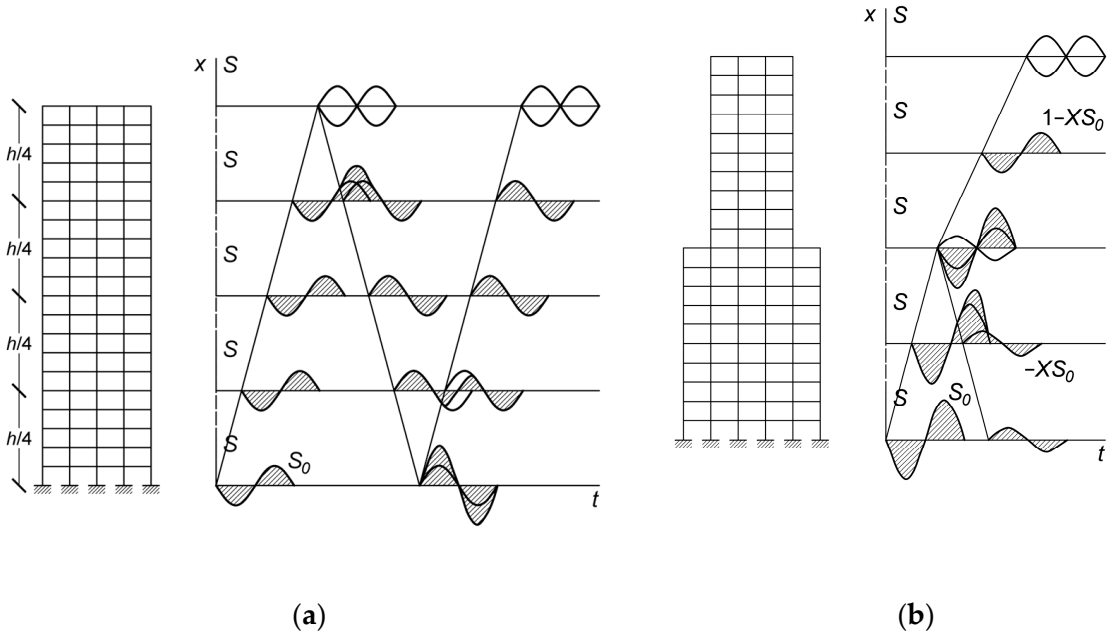

(**a**) (**b**)

Figure 6. Shear transmission inside a building, based on [20,21]: (**a**) building with constant stiffness and mass in relation to height; (**b**) effect of reflection due to a change in stiffness.

For changes in the lateral stiffness between floors, it was assumed that part of the wave was reflected and part was transmitted (Figure 6b). For a wave moving upward, the shear wave was reflected in the ratio $-X$ and was transmitted in the ratio $1 - X$. And for a wave moving downward, the ratios of reflection and transmission were X and $1 + X$, respectively. The ratio X can be calculated using Equation (12), where K_1 is the stiffness of the story where the wave comes from, and K_2 is the stiffness of the story where the wave goes; c_1 and c_2 are the weights of the floors with an analogous definition for the subscripts. A demonstration of Equation (12) can be found in [20,21]. For the analysis of the superposition of waves, only the transmitted part of the waves was considered. Besides the reflected waves at the base and at the top of the structure, the reflected waves inside the structure were neglected. Also, changes in the velocity of the wave transmission due to changes in the stiffness were not considered.

$$X = \frac{\sqrt{K_1 c_1} - \sqrt{K_2 c_2}}{\sqrt{K_1 c_1} + \sqrt{K_2 c_2}} \tag{12}$$

To account for energy dissipation, the amplitude of the reflected waves at the top and base of the structure were reduced by 5% and 10%, respectively. The analysis of the superposition of waves was first performed based on a ground motion of amplitude S_0, a two-second period and four continuous cycles. It was found that the maximum story shears occurred during the transient response of the structure, and therefore, four cycles were sufficient for the analysis. The graphical representation of the described analysis for a structural period of 2.36 s (fundamental modes) is depicted in Figure 7. The maximum shear was calculated only for the levels 1, 3, 5 and 13, and the results were $3.8S_0$, $3.2S_0$, $2.2S_0$ and $0.95S_0$, respectively. The shear for the remaining levels was obtained by interpolation.

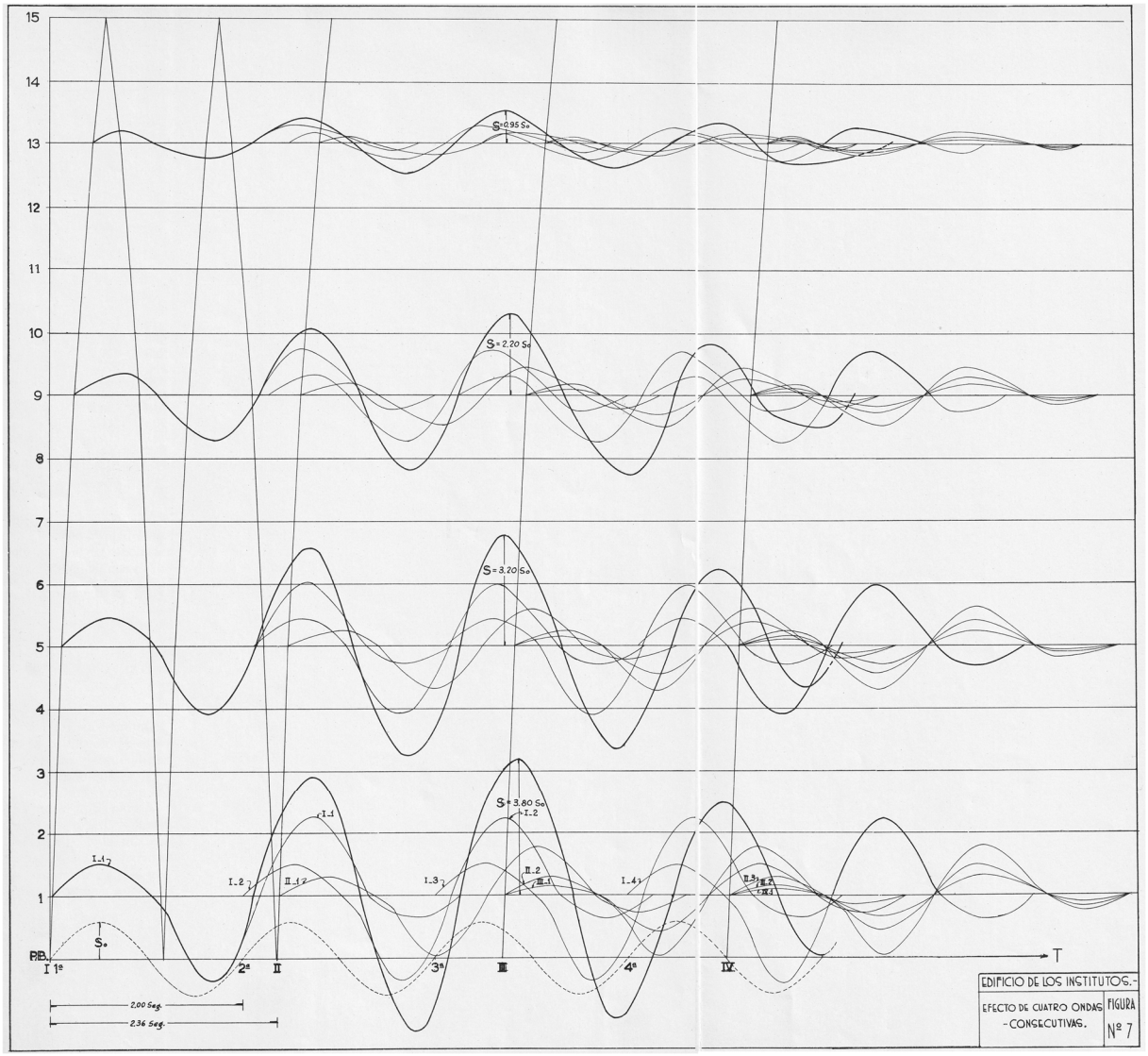

Figure 7. Analysis of superposition of shear waves inside the building for a structural period of 2.36 s and ground motion with period of 2.00 s [20].

A second analysis was then performed using a ground motion with period of one second. No graphical representation of these results was reported, so it is not clear if the structural period was considered as 2.36 s (fundamental modes) or 1.00 s (second longitudinal mode). However, from this analysis, story shears of greater magnitude were found for the three upper stories. The design shear for each story was finally defined as the maximum of the two previously described analyses.

4. Ambient Vibration Tests

Ambient vibration tests were performed during the structural assessment of the building to determine its principal vibration modes and modal shapes [27]. The instrumentation consisted of six triaxial accelerometers, eight uniaxial accelerometers, five six-channel digitizers and a controller for the instrument operation and the data acquisition. A total of 23 record points was used; 1 point was in the ground around the building, while the rest were inside the building (Figure 8). Four tests with different accelerometer arrangement were carried out. Each test had a duration of 30 min with a sampling frequency of 100 Hz.

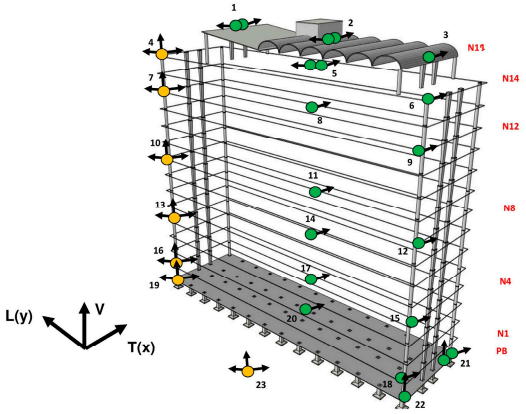

Figure 8. Location of record points for the ambient vibration tests [27], triaxial accelerometers in yellow and uniaxial accelerometers in green.

The signal analysis allowed us to identify the first three vibration modes of the building in the transverse, longitudinal and torsional/rotational directions (Table 5). In addition, three modes of the 15th floor were identified, which confirmed the appendix-like behavior of this floor. Modal shapes corresponding to the first six modes are shown in Figure 9. Furthermore, from the comparison of the records obtained for the base of the structure and the surrounding ground, it was found that the transference function is closer to one in the range of frequencies between 0.8 and 10.0 Hz. Therefore, the soil–structure interaction effects can be neglected in the response of the building.

Table 5. Mean vibration frequencies and periods identified from ambient vibration tests [27].

Mode	Vibration Frequencies (Hz)			Vibration Periods (s)		
	Longitudinal Direction (L)	Transverse Direction (T)	Torsional Direction (R)	Longitudinal Direction (L)	Transverse Direction (T)	Torsional Direction (R)
1	0.635	0.586	0.714	1.57	1.71	1.40
2	1.801	1.819	2.228	0.56	0.55	0.45
3	3.174	3.284	4.257	0.32	0.30	0.23
Level 15	6.005	3.308	5.298	0.17	0.30	0.19

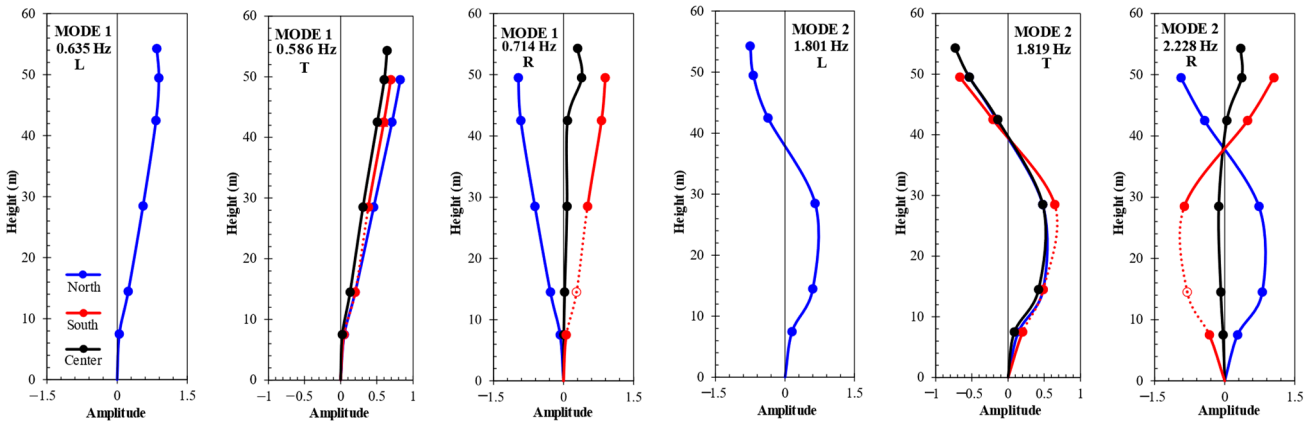

Figure 9. Modal shapes of the first six vibration modes identified from ambient vibration tests [27].

The fundamental vibration mode appears in the transverse direction, followed by a translational mode in the longitudinal direction and a torsional mode. This result differs from the design results, where both vibration modes were associated with the same value. Therefore, the structure is stiffer in the longitudinal direction than in the transverse direction.

However, the periods for the second and third modes are closer in both directions. The order of the modes also shows the global regularity of the structure.

Note that the results of ambient vibration tests indicate that the structure is stiffer than the estimated model from design methods. The fundamental period based on ambient vibration is 28% less than the fundamental period from Table 2 (2.36 s). This means that the physical stiffness of the structure is approximately 90% greater than the design estimation. Two main sources of stiffness underestimation during the design were identified: first, differences in the dimensions of the structural elements considered during the design versus the measured dimensions (see Table 1); second, the stiffness contribution of structural and non-structural walls.

5. Numerical Modeling

Two numerical models were performed with the aim of reproducing the vibration periods of the building obtained from the design methods and the ambient vibration tests, respectively (Figure 10). Both models were developed using commercial software, ETABS [28], with the following general assumptions:

- The geometry was modeled in three dimensions;
- Beams and columns were modeled by means of beam elements with non-cracked sections;
- Floor systems were considered as rigid diaphragms;
- The eccentricity of longitudinal beams located in the B and C axes was not considered; therefore, all beams in a floor had the same elevation;
- The columns were fixed at their bases, and the foundation elements were not included.

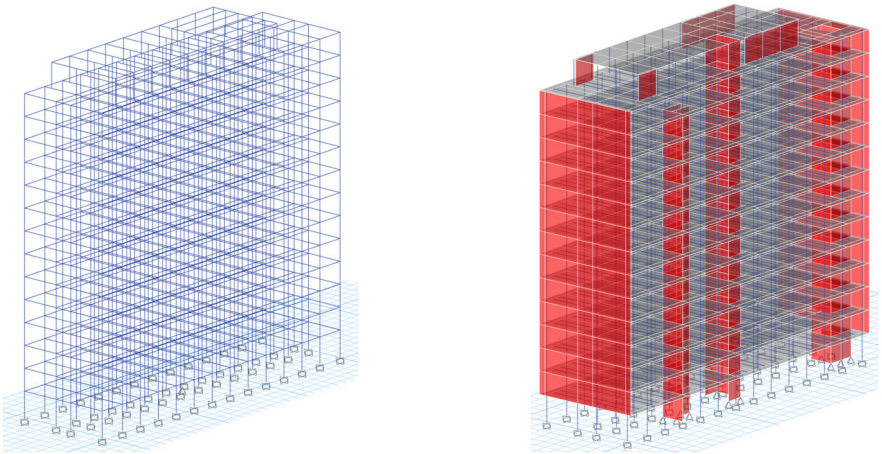

(**a**) (**b**)

Figure 10. Numerical models: (**a**) model 1, for reproducing design results; (**b**) model 2, for reproducing results of ambient vibration.

5.1. Numerical Model 1

The first model developed was in accordance with the assumptions described in [20]. This implied the following additional assumptions:

- Only columns and principal beams were modeled;
- The dimensions of columns and beams reported in the design were used;
- All the beam sections were considered with rectangular geometry;
- The stiffness contribution of masonry walls was neglected;
- A concrete elasticity modulus of 20,000 MPa was used;
- Floor masses from the design were considered to be lumped in the center of mass of each floor as translational masses in the transverse and longitudinal directions.

The obtained results are summarized in Table 6. The vibration periods for the longitudinal direction do not differ more than 7% from the design values. In the transverse direction, this difference increases up to 34%. In both cases, the numerical model produces a more flexible structure compared to the design estimation; however, the accuracy of the design procedures for the longitudinal direction must be highlighted.

Table 6. Frequencies and periods obtained from numerical model 1.

Mode	Frequency (Hz)	Period (s)	Model 1 Period/Design Period	Description
1	0.317	3.15	1.34	1st transverse
2	0.405	2.47	1.05	1st longitudinal
3	0.906	1.10	-	2nd transverse
4	0.944	1.06	1.07	2nd longitudinal

Based on a review of the procedure used to calculate the transverse period, it has been found that the main source of error is due to differences in the internal forces obtained during the structural analysis of the typical transverse frame. Although the solution obtained during the design is statically consistent, the approximate method used is based on hypotheses that are not necessarily fulfilled. On the other hand, the imposition of a lateral load distribution for the transverse direction analysis was the source of an additional error. It is well known that the lateral stiffness of a structure depends on the lateral load distribution.

Figure 11 shows the lateral stiffnesses of a typical transverse frame according to design methods and numerical model 1. The stiffnesses of the numerical model were obtained from the analysis of a 2D frame, which was isolated from the whole model, and were subjected to the same lateral load distribution considered in the design procedures. It can be seen that the design method overestimates the stiffness of the frame, in accordance with the comparison of vibration periods. The maximum overestimation is 130% and occurs on the ninth floor.

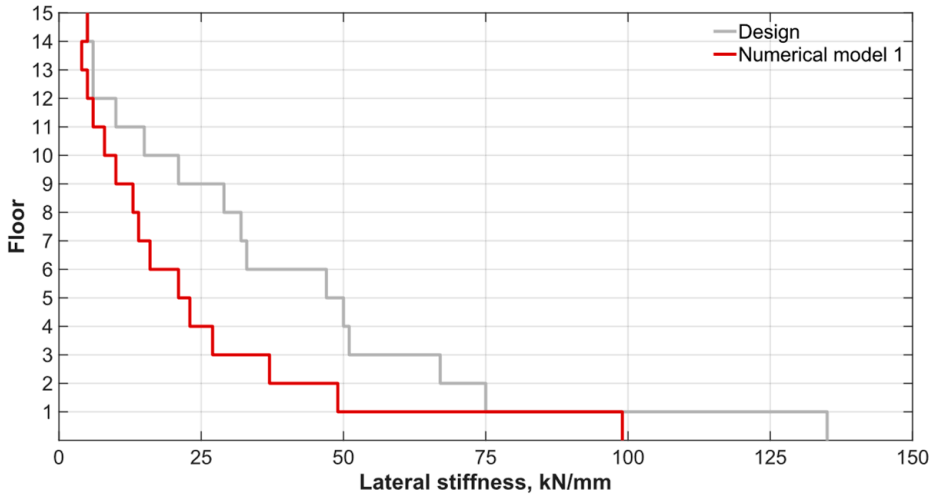

Figure 11. Lateral stiffness of a typical transverse frame based on design methods and numerical model 1.

The comparison of the modal shapes is shown in Figure 12. All modal shapes have been adjusted to a unitary amplitude on the top floor. From a qualitative point, the modal shapes are equal for the first mode in both directions. In the case of the second longitudinal modal shape, slight discrepancies can be noted for most of the floors. These observations were confirmed quantitatively by calculating the sum of the squares of the errors. The

values obtained were 0.018, 0.004 and 0.291 for the first transverse, first longitudinal and second longitudinal modes, respectively.

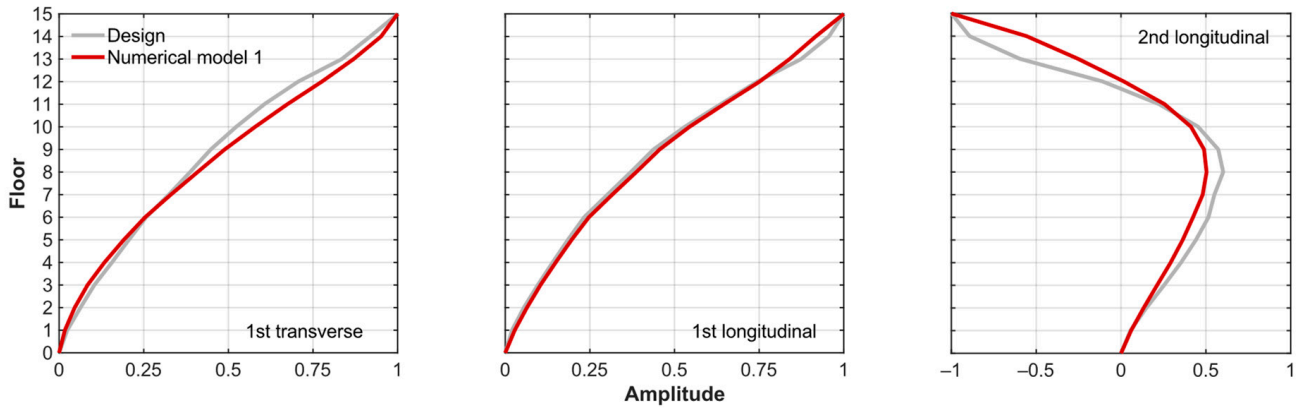

Figure 12. Modal shapes according to design method [20] and numerical model 1.

5.2. Numerical Model 2

The second model was developed as part of the structural assessment process of the building. The characteristics of the model were defined on the basis of the original architectural and structural drawings, information obtained from site surveys and results from structural tests. The above could be summarized with the following assumptions:

- In addition to columns and principal beams, secondary beams and masonry walls were modeled;
- Measured dimensions of columns and beams were used;
- The cross-sections of principal beams included the effective portion of the lower slab monolithically casted with the beams;
- Masonry walls were modeled using "shell thin" area elements;
- The box-type floor system was modeled by a single slab using "membrane" area elements that did not affect the stiffness of the system and were only used to distribute loads to the beams;
- On the 15th floor, barrel vaults were modeled as horizontal slabs using "membrane" area elements;
- The portion of the line elements within the beam–column joints were considered as semi-rigid elements for flexure;
- Elasticity modules for concrete (15,800 MPa), clay masonry walls (3600 MPa) and sand–cement masonry walls (3200 MPa) were obtained using a calibration procedure to approximate the numerical results to the experimental ones;
- Live loads were defined according to the mean values given in the current Mexican Code for actions definition [29]; these values were considered acceptable based on the observed use of the building during the ambient vibration tests.

The obtained results are summarized in Table 7. Only the modes for comparison with the experimental results are shown. It should be noted that the numerical model accurately reproduces the order of the ambient vibration, except for the exchange of the third torsional and the torsional appendix modes. The differences in the numerical periods from the experimental values are not greater than 15% for the first eight modes. For the first three modes, which have mass participation factors around 70% in their respective directions, the differences are less than 5%. On the other hand, it is observed that the larger deviations between the numerical and experimental results are found in the third torsional and the longitudinal appendix modes. In general, the numerical model underestimates the torsional periods of the experimental results.

Table 7. Vibration frequencies and periods obtained from numerical model 2.

Mode	Frequency (Hz)	Period (s)	Model 2 Period/ Experimental Period	Description
1	0.570	1.76	1.03	1st transverse
2	0.623	1.61	1.02	1st longitudinal
3	0.743	1.35	0.96	1st torsional
4	1.656	0.60	1.09	2nd longitudinal
5	1.927	0.52	0.94	2nd transverse
6	2.613	0.38	0.85	2nd torsional
7	2.955	0.34	1.07	3rd longitudinal
8	3.641	0.28	0.90	3rd transverse/transverse appendix
11	4.864	0.21	0.88	Torsional appendix
13	5.594	0.18	0.76	3rd torsional
19	9.348	0.11	0.64	Longitudinal appendix

A comparison of the modal shapes for the translational modes is shown in Figures 13 and 14. It can be observed that the modal shapes are in good agreement in both directions for the first and second modes. On the other hand, some differences in the amplitude are observed in the modal shapes for the third modes, although the location of inflection points can be considered as coincidental. The sum of the squares of the errors was again calculated but only considering the amplitude of the floors where experimental results were obtained. For the transverse modes, the values obtained were 0.004, 0.068 and 0.272 for the first to third modes. For the longitudinal modes, the values obtained were 0.029, 0.094 and 0.435 for the same order of modes. These results show a better approximation for the transverse modes than for the longitudinal modes. In addition, it is clear that the amount of error increases for the higher modes.

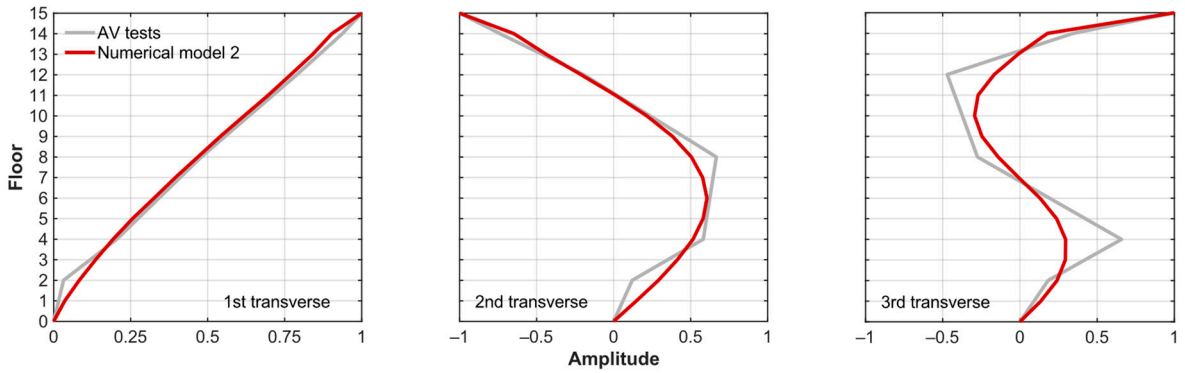

Figure 13. Modal shapes for transverse translational modes according to ambient vibration tests (AV tests) and numerical model 2.

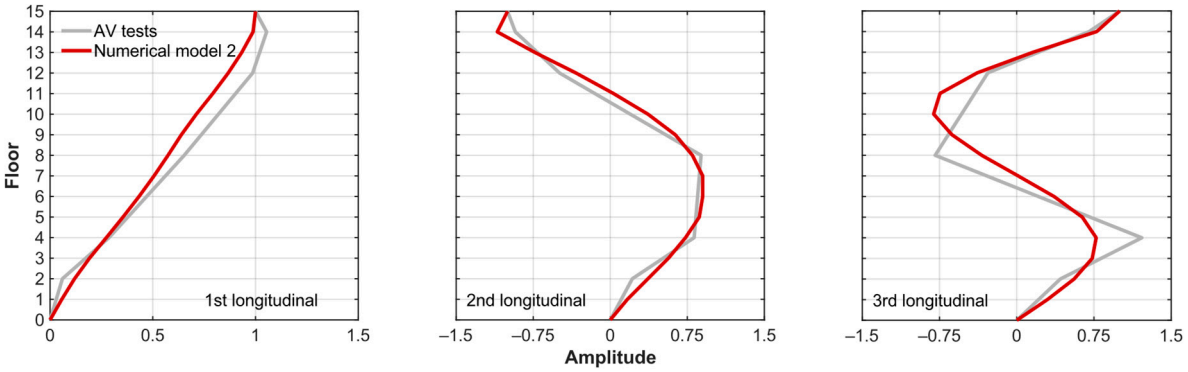

Figure 14. Modal shapes for longitudinal translational modes according to ambient vibration tests (AV tests) and numerical model 2.

6. Conclusions

This paper reviewed the methodology used for the seismic design of a reinforced concrete moment frame building, built in the middle of the 20th century, which is considered part of Modern Heritage. The methodology is of particular interest, as it involves the application of pioneer concepts of dynamic analysis in the design of tall buildings in Mexico in the 1950s. The procedure can be summarized in three stages: (1) the estimation of the dynamic properties of the structure; (2) the definition of the idealized harmonic ground movement in terms of period and maximum acceleration; (3) the analysis of the superposition of shear waves within the structure for the calculation of the maximum shear at each story.

The review, which includes a comparison between the dynamic properties estimated during the design and those obtained from recent ambient vibration tests and numerical models, allowed us to identify important design criteria of that time. It was shown that the fundamental period of the structure, which is a key aspect of seismic analysis, overestimated the experimental results by 38%. This finding implies subsequent errors in the calculation of story shears and significant uncertainty in the design. Differences in the vibration periods were a consequence of a global underestimation in the lateral stiffness of the structure. Four sources of error were identified regarding the stiffness calculation: (1) neglecting the stiffness contribution of the masonry walls; (2) considering elements with smaller dimensions compared to the physical ones; (3) using a larger elasticity modulus for the concrete compared to current specifications and (4) adopting the procedure in the transverse direction, as an alternative to the application of the Equation of Wilbur (1), due to the irregularity of the frames. It is worth noting that all the errors were not additive. Errors 1 and 2 produced an underestimation of the lateral stiffness, while errors 3 and 4 were sources of overestimation. However, the global result of the errors was the mentioned stiffness underestimation.

Besides the source of error 4, from the comparison between the design results and the numerical model 1, it was observed that the analytical methods adopted for the longitudinal direction were accurate according to the design assumptions. In contrast to trans-verse frames, longitudinal frames were regular, and the maximum difference of numerical vibration periods with respect to design values was only 7%. On the other hand, the difference in the transverse period was of significantly larger order (34%). This shows the limitations of the analysis methods of that time in the presence of irregular structures.

In the case of numerical model 2, which was aimed at reproducing the vibration ambient results, it was shown that numerical modeling is an excellent tool for representing the dynamic behavior of a building. Although the model was maintained simply, by avoiding the explicit modeling of the unusual floor system of the building, the results were sufficiently accurate. Therefore, this calibrated model was used as the basis for the numerical revisions in the structural assessment. However, it must be highlighted that the validity of a numerical model can only be established by means of a calibration process using the result from site tests, as is the case for ambient vibration tests. Only on this basis it is possible to select the most suitable modeling approach.

Overall, the review presented in this paper allowed us to illustrate the evolution of seismic analysis overtime and show, with detail, the common design criteria for a specific period of time. This information improves the recognition of the intrinsic engineering value of similar buildings, including those considered as part of Modern Heritage. It can be observed that additional research is needed to further analyze the implications of the design criteria on the structural safety of the building under study, for example, the evaluation of the change in the story shears due to the error in the estimation of vibration periods and how these forces compare to those obtained using current methods and design codes.

Author Contributions: Conceptualization, F.P. and J.R.; methodology, F.P. and J.R.; software, J.R.; validation, F.P. and J.R.; formal analysis, J.R.; investigation, J.R.; resources, F.P.; data curation, J.R.; writing—original draft preparation, F.P. and J.R.; writing—review and editing, F.P. and J.R.; visualiza-

tion, J.R.; supervision, F.P.; project administration, F.P.; funding acquisition, F.P. All authors have read and agreed to the published version of the manuscript.

Funding: This research received no external founding.

Data Availability Statement: The original contributions presented in the study are included in the article, further inquiries can be directed to the corresponding author.

Acknowledgments: The authors are grateful to the Dirección General del Patrimonio Universitario and the Dirección General de Obras y Conservación, both of the Universidad Nacional Autónoma de México (UNAM), for their assistance during the process of structural assessment. We also acknowledge the group of David Murià† of the Instituto de Ingeniería, UNAM, especially Gerardo Rodríguez and M.I. Miguel Leonardo, for the execution and interpretation of the ambient vibration tests.

Conflicts of Interest: The authors declare no conflicts of interest.

Nomenclature

a	Amplitude of the ground motion idealized as a harmonic signal
C	Weight of the first floor of the structure
C_1	Weight of the floor where the wave comes from (for calculation of X)
C_2	Weight of the floor where the wave goes (for calculation of X)
c	Weight per unit of height for an idealized structure with constant weight in height
E	Elasticity modulus
E_c	Elasticity modulus of concrete
f	Mathematical function two-times derivable
f'_c	Concrete compressive strength
g	Gravity acceleration
H	Total height of the structure
h	Story height
K	Lateral stiffness per unit of height for an idealized structure with constant lateral stiffness in height
K_1	Lateral stiffness of the story where the wave comes from (for calculation of X)
K_2	Lateral stiffness of the story where the wave goes (for calculation of X)
K_{co}	Inertia-to-length relation of each column of the n story
K_{ga}	Inertia-to-length relation of each upper beam of the n story
K_{gb}	Inertia-to-length relation of each lower beam of the n story
k	Lateral stiffness of the first story
k_n	Lateral stiffness of the n story
S	Story shear as a function of time and height
S_0	Shear at the base of the structure as a function of time
T	Period of the idealized ground motion
T_s	Vibration period of the structure
t	Time
X	Ratio for the calculation of reflection of waves in changes of lateral stiffness between consecutive floors of a structure
x	Height
y	Lateral displacement as a function of time and height
y_0	Ground motion idealized as a harmonic signal
ω	Circular frequency of the idealized ground motion

References

1. ICOMOS. Principles for the Analysis, Conservation and Structural Restoration of Architectural Heritage. 2003. Available online: https://iscarsah.org/wp-content/uploads/2014/11/iscarsah-principles-english.pdf (accessed on 7 September 2024).
2. ISCARSAH. Recommendations for the Analysis, Conservation and Structural Restoration of Architectural Heritage. 2003. Available online: https://iscarsah.org/wp-content/uploads/2023/01/part-ii-e28093-guidelines.pdf (accessed on 7 September 2024).
3. Lourenço, P.B. Recommendations for restoration of ancient buildings and the survival of a masonry chimney. *Constr. Build. Mater.* **2006**, *20*, 239–251. [CrossRef]
4. Vinh, A.L.; Dinh, S.C. Study on Vietnamese design methods of traditional vernacular architecture and discussion on their technical origins. *Int. J. Archit. Herit.* **2024**, *4*, 622–651. [CrossRef]

5. Gaetani, A.; Monti, G.; Lourenço, P.B.; Marcari, G. Design and analysis of cross vaults along history. *Int. J. Archit. Herit.* **2016**, *10*, 841–856. [CrossRef]
6. Moreno, P. Rodrigo Gil de Hontañón and 16th-century building techniques: The Cimborio Vault of Archbishop Fonseca College Chapel in Salamanca (Spain). *Int. J. Archit. Herit.* **2016**, *10*, 1110–1124. [CrossRef]
7. Cavalagli, N.; Gusella, V. Structural investigation of 18th-century ogival masonry domes: From Carlo Fontana to Bernardo Vittone. *Int. J. Archit. Herit.* **2015**, *9*, 265–276. [CrossRef]
8. De Stanis, S.; De Felice, G. Overview of railway masonry bridges with a safety factor estimate. *Int. J. Archit. Herit.* **2014**, *8*, 452–474. [CrossRef]
9. Brencich, A.; Mordbiducci, R. Masonry arches: Historical rules and modern mechanics. *Int. J. Archit. Herit.* **2007**, *1*, 165–189. [CrossRef]
10. Schueremans, L.; Porcher, H.; Rossi, B.; Wouters, I.; Verstrynge, E. A study on the evolution in design and calculation of iron and steel structures over the mid 19th century in western and central Europe. *Int. J. Archit. Herit.* **2018**, *12*, 320–333. [CrossRef]
11. Peña, F.; Manzano, J. Dynamical characterization of typical Mexican colonial churches. In *Seismic Assessment, Behavior and Retrofit of Heritage Buildings and Monuments*; Psycharis, I.N., Pantazopoulou, S.J., Papadrakakis, M., Eds.; Computational Methods in Applied Sciences; Springer: Berlin/Heidelberg, Germany, 2015; Volume 37, pp. 297–319, Chapter 12. [CrossRef]
12. Gültekin, E. *Heritage and Preservation of Modern Architecture*; National Technical University of Athens: Athens, Greece, 2019. [CrossRef]
13. Pizzigatti, C.; Franzoni, E. The problem of conservation of XX century architectural heritage: The fiberglass dome of the woodpecker dance club in Milano Marittima (Italy). *J. Build. Eng.* **2021**, *42*, 102476. [CrossRef]
14. Macdonald, S. 20th-Century Heritage: Recognition, Protection and Practical Challenges. *Herit. Risk* **2003**, 223–229.
15. Conti, A. Modern heritage and the World Heritage Convention. *World Herit.* **2017**, *85*, 8–17.
16. Muslimin, R. Rule-based design analysis and structural rationalization study of Ralph Symonds laminated timber arches. *Int. J. Archit. Herit.* **2023**, *10*, 1669–1684. [CrossRef]
17. Rosenblueth, E. Aseismic design in Mexico. In Proceedings of the 1st World Conference on Earthquake Engineering, Berkeley, CA, USA, June 1956.
18. Rosenblueth, E. Aseismic provisions for the Federal District, Mexico. In Proceedings of the 2nd World Conference on Earthquake Engineering, Tokyo and Kyoto, Japan, 11–18 July 1960.
19. *Reglamento de las Construcciones y de los Servicios Urbanos en el Distrito Federal*; Diario Oficial de la Federación: Mexico City, Mexico, 1942.
20. Escalante, C. *El Análisis Dinámico de la Torre de Ciencias de la Ciudad Universitaria de México*; Ediciones ICA: Mexico City, Mexico, 1951.
21. Westergaard, H. Earthquake-shock transmission in tall buildings. *Eng. News Rec.* **1933**, *111*, 654–656.
22. Newmark, N.M. Numerical procedure for computing deflections, moments and buckling loads. *Trans. ASCE* **1942**, *2202*, 1161–1234. [CrossRef]
23. Rosenblueth, E.; Esteva, L. *Folleto Complementario: Diseño Sísmico de Edificios*; Ediciones Ingeniería: Mexico City, Mexico, 1962; pp. 54–56.
24. Cross, H.; Dolbey, N. *Continuous Frames of Reinforced Concrete*; John Wiley and Sons, Inc.: New York, NY, USA, 1932; pp. 221–236.
25. Kidder, F.; Parker, H. *Kidder-Parker Architects' and Builders' Handbook*, 18th ed.; John Wiley and Sons, Inc.: New York, NY, USA, 1956.
26. Norma Técnica Complementaria para Diseño y Construcción de Estructuras de Concreto. Gaceta Oficial de la Ciudad de México: Mexico City, Mexico, 2023. Available online: https://data.consejeria.cdmx.gob.mx/portal_old/uploads/gacetas/b3c4f4ff37241d0a93cc6742a8b0bf2f.pdf (accessed on 14 September 2024).
27. Leonardo, M.; Rodríguez, G.; Murià, D. *Estudio de Vibración Ambiental en la Torre de Humanidades II en Ciudad Universitaria, Apoyo al Programa de Seguridad Estructural de las Construcciones Patrimoniales de la UNAM 2021–2023*; Instituto de Ingeniería de la UNAM: Mexico City, Mexico, 2023.
28. Computers and Structures, Inc. *CSI Analysis Reference Manual, ETABS V20 Analysis and Design of Buildings Systems*; Computers and Structures, Inc.: New York, NY, USA, 2017.
29. Norma Técnica Complementaria sobre Criterios y Acciones para el Diseño Estructural de las Edificaciones. Gaceta Oficial de la Ciudad de México: Mexico City, Mexico, 2023. Available online: https://www.obras.cdmx.gob.mx/storage/app/media/Normas%20tecnicas/NTC-2023.pdf (accessed on 14 September 2024).